

**AN ALGORITHM FOR CALCULATING THE PLUME
CENTERLINE TEMPERATURE IN THE PRESENCE OF A HOT
UPPER LAYER**

by

**William D. Davis and Kathy A. Notarianni
Building and Fire Research Laboratory
National Institute of Standards and Technology
Gaithersburg, MD 20899 USA**

And

**Phillip Z. Tapper
Goddard Space Flight Center
National Aeronautics and Space Administration
Greenbelt, MD 20771 USA**

Reprinted from Journal of Fire Protection Engineering, Vol. 10, No. 3, 23-31, 2000

NOTE: This paper is a contribution of the National Institute of Standards and Technology and is not subject to copyright.

NIST

National Institute of Standards and Technology
Technology Administration, U.S. Department of Commerce

AN ALGORITHM FOR CALCULATING THE PLUME CENTERLINE TEMPERATURE IN THE PRESENCE OF A HOT UPPER LAYER

William D. Davis and Kathy A. Notarianni
Building and Fire Research Laboratory
National Institute of Standards and Technology
Gaithersburg, MD 20899

Phillip Z. Tapper
Goddard Space Flight Center
National Aeronautics and Space Administration
Greenbelt, MD 20771

ABSTRACT

The analysis of recent experiments using JP-5 and JP-8 pool fires performed in 15 m and 22 m high hangars suggests that plume centerline temperature correlations found in the computer fire model FPEtool underpredict the ceiling temperature for large fires. The analysis was based on the results of thirty-three fire tests which had heat release rates ranging from 100 kW to 33 MW and ambient temperatures ranging from 8°C to 31°C. It is shown that using Evans' virtual source method, coupled with a radiative fraction correlation that depends on pool diameter, provides plume centerline temperature predictions that agree with experiment. When an upper layer does not form, Heskestad's correlation provides good agreement with the measured plume centerline temperatures.

INTRODUCTION

Recent experiments conducted in hangars with ceiling heights of 15 m and 22 m provided a test bed for computer model comparisons with ceiling jet temperatures, plume centerline temperatures, and predictions of detector activations.¹ A comparison of the models in FPEtool Version 3.2² with the experimental data indicated that the predictive capabilities of the models were not in agreement with the experimental results when hot upper layers were present. This observation has led to the development of an improved model to predict plume centerline temperatures.

The experiments were designed to provide insight into the behavior of jet fuel fires in aircraft hangars and to study the impact of these fires on the design and operation of a variety of fire protection systems. As a result, the test series included small fires designed to investigate the operation of UV/IR detectors and smoke detectors as well as large fires which were used to investigate the operation of ceiling mounted heat detectors and sprinklers. The impact of the presence or absence of draft curtains was also studied in the 15 m hangar.

It is shown that, in order to predict the plume centerline temperature within experimental uncertainty, the entrainment of the upper layer gas must be modeled. For large fires, the impact of a changing radiation fraction must also be included in the calculation.

EXPERIMENTS

Two experimental sites were used to conduct the hangar experiments. The first site was a warm temperature site (~ 30°C) at Barbers Point, Hawaii and the second site was a cool temperature site (~ 12°C) at Keflavik, Iceland.

The Barbers Point Experiments

At the Barbers Point site, a total of eleven fire experiments were conducted. Six of the experiments included a draft curtain, 3.7 m deep, which enclosed an area of dimensions 18.3 m x 24.4 m. The hangar measured 97.8 m x 73.8 m in area and had a ceiling height at the center of 15.1 m. The ceiling height at the center of the draft curtained area was 14.9 m. As an aid in describing the experimental setup, the directions east and west will be used to describe directions

pointing parallel to the 24.4 m side of the draft curtain while north and south will be used to describe directions perpendicular to the 24.4 m side. A plan view of the hangar bay is shown in Fig. 1.

The hangar roof consists of built-up tar and gravel over a corrugated metal deck. The roof slopes from a height of 15.1 m at the center toward the east and west walls which are 13.4 m high. The metal deck is directly supported by 0.25 m I-beams which run the (N-S) width of the hangar and are spaced 4.1 m on center. The I-beams are supported by open steel trusses which run perpendicular to the beams (E-W) and are spaced 6.1 m on center. These trusses span the full length of the hangar.

Three of the six draft curtain experiments developed sufficiently large excess temperatures at the ceiling to provide a useful test bed for the development of ceiling jet correlations (separate study). The experimental fires were 1.5 m, 2.0 m, and 2.5 m diameter JP-5 pan fires which produced steady state heat release rates (HRR) of 2.8 MW, 6.8 MW, and 7.7 MW respectively. The heat of combustion of JP-5 is 43 MJ/kg.¹ Due to a load cell failure, the heat release rate for the 2.5 m diameter fire was calculated from the average mass loss over the duration of the fire. The average mass loss was determined by measuring the initial and final volume of fuel contained in the pan and multiplying the volume difference by the fuel density to determine the fuel mass consumed by the fire. Estimates of HRR using the average mass loss agreed to within 20%, on average, with the HRR calculated directly from the load cell measurements.

The fire plume in the 6.8 MW experiment developed a fire whirl at two different times during

the experiment. The existence of these plume whirls not only impacted the characteristics of the plume temperature but also produced distinct changes in the layer temperature time history. As a result, this experiment will not be included in the analysis. All the other experiments produced normal fire plumes.

Two experiments, which did not include draft curtains, developed sufficiently large excess temperatures at the ceiling to be useful in studying the unconfined ceiling jet. These fires were 2.0 m and 2.5 m diameter JP-5 pan fires with steady state heat release rates of 5.6 MW and 7.7 MW. The 5.6 MW heat release rate was calculated using the average mass loss over the duration of the fire while the 7.7 MW heat release rate was assumed to be equal to the estimated heat release rate of the 2.5 m diameter pan fire with draft curtains since average mass loss data was not available for this test.

Thermocouples were used to measure the plume temperature and ceiling jet temperature at radial distances from plume center of 0.0 m, 1.5 m, 3.0 m, 6.1 m, 9.1 m, and 11.6 m in the experimental east and west directions, and at 1.5 m, 3.0 m, 6.1 m, and 8.5 m in the experimental north and south directions. The thermocouples were located 0.31 m beneath the ceiling. The r/H value (r is the radial distance from the plume center and H is the height of the ceiling above the fire surface) for the 1.5 m thermocouples is 0.1 which means that these thermocouples are in the plume. All the other thermocouples were located outside the plume region. Four thermocouple trees with thermocouples located at 0.15 m, 0.3 m, 0.46 m, 0.61 m, and 0.76 m beneath the ceiling were located 6.1 m from plume center in the north, south, east, and west directions, while a fifth tree with thermocouples located at 0.15 m, 0.3 m, 0.46 m, 0.76 m, 1.22 m, and 3.0 m beneath the ceiling was located at 9.1 m toward experimental east. These thermocouple trees are used to investigate the temperature dependence of the ceiling jet as a function of distance beneath the ceiling (measurements for a separate study).

The Keflavik Experiments

A total of 21 pan fire experiments were conducted at Keflavik, Iceland. The Keflavik hangar measured 73.8 m by 45.7 m and had a barrel roof

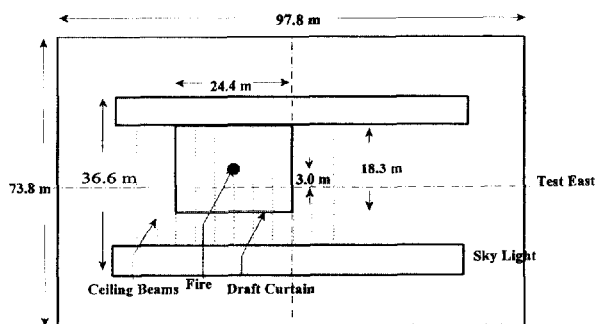


Figure 1. Plan view of 15 m hangar bay.

which was 22.3 m high at the center and 12.2 m high at the walls. Corrugated steel draft curtains were used to divide the ceiling into five equal bays approximately 14.8 m by 45.7 m with the fire experiments conducted in the middle bay and centered under the 22.3 m high ceiling.

The primary roof support consisted of a series of steel trusses which form arches spanning the width of the hangar bay, running parallel to the hangar doors. These primary trusses are approximately 1.0 m deep and are spaced 7.4 m on center. The primary trusses are interconnected with a series of secondary trusses which are perpendicular to them and run the length of the hangar bay. The secondary trusses are spaced at intervals ranging from 5.8 m to 6.4 m on center. The metal deck roof is directly attached to a series of steel beams which sit on top of the primary and secondary trusses. These steel beams are perpendicular to the primary trusses, are spaced 1.5 m to 2.1 m on center, and vary in height from 0.2 m to 0.3 m.

The roof was insulated via a barrel shaped suspended tile ceiling which was supported by a conventional suspended tile ceiling grid located at the same elevation as the bottom of the steel beams. The individual ceiling tiles in the center bay and the adjacent bay were removed prior to testing.

Experimental east and west were designated to be the directions parallel to the draft curtain located 13.4 m above the floor and pointed along the direction of the barrel roof. Experimental north and south directions ran perpendicular to the draft curtain. Thermocouples located 0.31 m beneath the ceiling were at radial distances from fire center of 0.0 m, 3.0 m, 4.6 m, 6.1 m, and 6.7 m in the south direction and 3.0 m and 6.1 m in the north direction. Thermocouples located 0.31 m beneath the ceiling were at radial distances from fire center of 3.0 m, 6.1 m, 9.1 m, 12.2 m, and 15.2 m in both the east and west directions and also at 18.3 m and 22.9 m in the east direction. Additional thermocouples were located at many of these locations and are represented in Fig. 2.

Twelve of the twenty-one experiments were not included in the analysis due to small fire size or windy conditions within the hangar. Of the

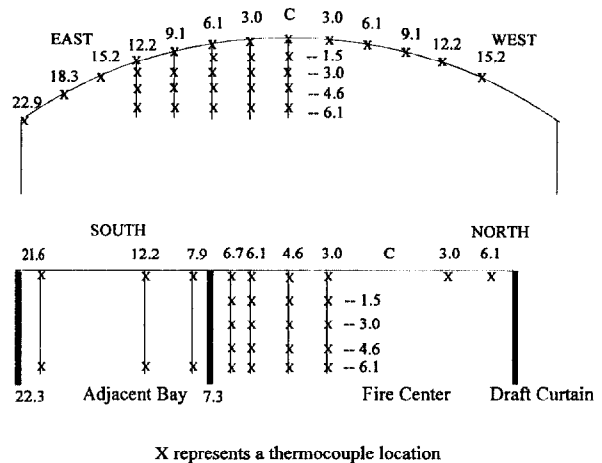


Figure 2. Thermocouple locations (in m) for the hangar at Keflavik.

remaining nine experiments, two were JP-5 round pan fires of diameters 2.0 m and 2.5 m with heat release rates 4.9 MW and 7.9 MW, respectively, while the other seven were square pan fires with sides of 0.9 m, 1.2 m, 3.0 m, and 4.6 m*. The steady state heat release rates for these fires ranged from 1.4 MW to 33 MW. The 14.3 MW fire was a JP-8, 3.0 m square pan fire while all the other fires were JP-5 square pan fires. The heat of combustion for JP-8 is 43 MJ/kg.¹ The heat release rates for all the Keflavik tests except the 33 MW fire test were measured using load cells. The heat release rate for the 33 MW fire was estimated based on pan surface area since the load cell would not support the pan.

PLUME CENTERLINE TEMPERATURE

The analysis of fire plumes is based on the solution of the conservation laws for mass, momentum and energy. Early work centered on point sources and assumed that the air entrainment velocity at the edge of the plume is proportional to the local vertical plume velocity.³ Measurements of plume centerline temperature in plumes with unconfined ceilings led to a correlation developed by Heskestad.⁴ The correlation gives the excess temperature as a function of height above a virtual point source to be

*Square pan fires were used for UV/IR detector tests to replicate standard industry fire pan sizes.

$$\Delta T = 9.1 \left(\frac{T_\infty}{g c_p \rho_\infty} \right)^{1/3} Q_c^{2/3} (z - z_0)^{-5/3} \quad (1)$$

The virtual origin is given by

$$z_0 = -1.02D + 0.083Q^{2/5} \quad (2)$$

where Q and Q_c are the total and the convective heat release rates, D is the pool diameter, z is the height above the fire surface, and T_∞ , c_p , and ρ_∞ are the temperature, heat capacity, and density of the ambient gas. The convective heat release rate is calculated by

$$Q_c = (1 - \chi_r)Q \quad (3)$$

where χ_r is the radiative fraction for the fire.

When a hot upper layer forms, this correlation must be modified in order to correctly predict plume centerline temperatures since the plume now includes added enthalpy by entraining hot layer gas as it moves through the upper layer to the ceiling. Methods involving defining a substitute virtual source and heat release rate applicable to the upper layer have been developed by Cooper⁵ and Evans.⁶ Evans' method is presently used in the computer fire model FPEtool.² This method defines the strength $Q_{I,1}^*$ and location $Z_{I,1}$ of the substitute source by

$$Q_{I,2}^* = [(1 + C_T Q_{I,1}^{*2/3}) / \xi C_T - 1 / C_T]^{3/2} \quad (4)$$

and

$$Z_{I,2} = \left[\frac{\xi Q_{I,1}^* C_T}{Q_{I,2}^{*1/3} [(\xi - 1)(\beta^2 + 1) + \xi C_T Q_{I,2}^{*2/3}]} \right]^{2/5} Z_{I,1} \quad (5)$$

$$Q_{I,1}^* = Q_c / (\rho_\infty c_p T_\infty g^{1/2} Z_{I,1}^{5/2}) \quad (6)$$

where $Z_{I,1}$ is the distance from the fire to the interface between the upper and lower layer, $Z_{I,2}$ is the distance from the substitute source to the layer interface, ξ is the ratio of upper to lower layer temperature, β is the velocity to temperature ratio of Gaussian profile half widths, and $C_T = 9.115$. The ceiling height for the substitute source is then obtained from

$$H_2 = H_1 - Z_{I,1} + Z_{I,2} \quad (7)$$

where H_1 is the location of the fire beneath the

ceiling. The values for the virtual fire source and ceiling height are then used in a standard plume correlation⁷ where the ambient temperature is now the temperature of the upper layer. The plume excess temperature is given by

$$\Delta T_p = 9.28 T_u (Q_{I,2}^*)^{2/3} \left(\frac{Z_{I,2}}{H_2} \right)^{5/3} \quad (8)$$

where T_u is the temperature of the upper layer.

RADIATIVE FRACTION

In order to model fire correctly, the radiative fraction of the heat release rate must be known. For large fires, the radiative fraction (χ_r) should decrease as fire size increases due to the increasing absorption path length with respect to the fire center and decreasing surface to volume ratio of the flame. A recent study of the effect of fire size on radiative fraction indicates that this effect may have a substantial impact on the calculation of plume centerline temperatures since, as the fire size increases, the radiative fraction decreases, allowing for more of the fire energy to heat the plume gases.⁹ Of particular interest is the variation of the radiative fraction for kerosene as a function of pan diameter. Based on a series of experiments,^{9,10,11} Yang et al.⁸ deduced that the radiative fraction for kerosene remained constant for pan diameters under 0.6 m but decreased rapidly for pan diameters between 2.0 m and 40.0 m ($\chi_r \propto D^{-0.6}$ where D is the pan diameter). No data was available for pan sizes between 0.6 m and 2.0 m. The jet fuel JP-5 is close to the composition of kerosene and would be expected to show a similar trend in radiative fraction.

In order to extend this correlation to pan diameters between 1.0 m and 2.0 m, the output signal from the IR detector portion of the combination UV/IR detectors located 21 m and 30 m from fire center divided by HRR was investigated for effective pan diameters ($\pi D^2/4 = \text{area}$) between 0.7 m and 5.2 m. The IR detector is sensitive to radiation which is emitted in a 0.6 μm wide band centered at 4.4 μm . The radiative fraction should be proportional to the number of counts/second/MW provided that the fraction of radiation emitted in this band compared to the total radiation emitted over all wavelengths is independent of pan diam-

eter. For pan diameters between 0.7 m and 1.5 m, the counts/second/MW was proportional to $D^{-0.7}$ and $D^{-0.5}$ for the IR detectors at 21 m and 30 m, respectively. This is in reasonable agreement with the dependence found for pan diameters between 2.0 m and 40.0 m.

The IR counts/second/MW fell off approximately inversely with pan diameter for the pan fires with diameters between 3.0 m and 5.2 m. Two reasons may account for this more rapid fall off of radiative fraction with increasing pan diameter. First, if the IR detectors did not see the changing flame height, this would lead to a linear dependence of counts/second/MW on pan diameter provided the emitting region resembled a cylindrical flame. The flame heights for the 3.0 m and 5.2 m diameter pan fires were observed to extend nearly to the hangar ceiling with intermittent flames being observed at the ceiling for the 5.2 m pan fire. Second, the fraction of radiation observed by the IR detectors may not be independent of pan diameter for sooty fuels such as JP-5. The average surface emissive power decreases as the pool diameter increases for diameters above 1.0 m. This decrease in surface emissive power is due to an increasing contribution of the radiation coming from soot.¹² Since soot tends to radiate most strongly at wavelengths shorter than $4.4 \mu\text{m}$ (the soot temperature is about 800 K^{12}), the IR detector used in this analysis should yield decreasing radiation fractions as the pan diameter increases. Both of these effects may play a role in the observed rapid fall-off in the counts/second/MW calculation for the larger pans.

For the calculations performed in the next section, it will be assumed that the fire diameter dependence of the radiative fraction of JP-5 is similar to kerosene. The radiative fraction for kerosene is estimated to be

$$\chi_r = 0.35*(2.0/D)^{0.6} \quad (9)$$

for pan diameters greater than about 1 m.

PLUME CENTERLINE TEMPERATURE COMPARISONS

Early in the fire experiments, prior to the development of the ceiling layer, the plume centerline temperature should follow the unconfined ceiling

correlation. As the ceiling layer develops, the impact of the layer on plume temperature should become evident as hot layer gases are entrained into the plume. Figure 3 shows the plume centerline temperature at approximately 200 s for eleven experiments. The first two experiments were conducted at Barbers Point and carry a "B" designator (ceiling height at fire location is 14.9 m), while the remainder were conducted at Keflavik (ceiling height at fire location is 22.3 m). All experiments used JP-5 except the one designated "8" in Keflavik which used JP-8. The total heat release rate is shown for each experiment. Also shown in the figure are the predictions of the plume correlation of Heskestad (Hesk), the plume model of Evans as calculated in Version 3.2 of FPEtool (FPEtool), and the prediction of the Evans' model (E-H&D) in LAVENT.¹³

The Evans' model was implemented as a side calculation in LAVENT. LAVENT was modified such that a user specified radiative fraction as a function of HRR could be input into the program. For the calculations reported in this paper, Eq. 9, which gives the radiative fraction as a function of pan diameter, was used to compute the radiative fraction for each pan size. LAVENT was then used to calculate the upper layer temperature and depth which supplied the necessary inputs for Evans' model, Eqs. 4-8. Evans' model was calculated in a separate subroutine of LAVENT which did not affect either the layer temperature or layer depth calculation. To obtain the plume centerline temperature, the strength and location of the substitute source were put into the correlation of Heskestad and Delichatsios⁷ which was evaluated at plume center. The modified version of LAVENT, designated as JET, is a test version and is not presently available.

Only the draft curtained area was modeled. This modeling assumption was reasonable early in the tests since both buildings were large enough that it required in excess of 200 s for the entire ceiling to fill with smoke down to the bottom of the draft curtains. The steady state heat release rate was used in each of the calculations.

The uncertainty intervals shown on the data in Fig. 3 represent one standard deviation as deduced from doing a least squares time average of five data points taken over a twenty second measurement period for the centerline thermo-

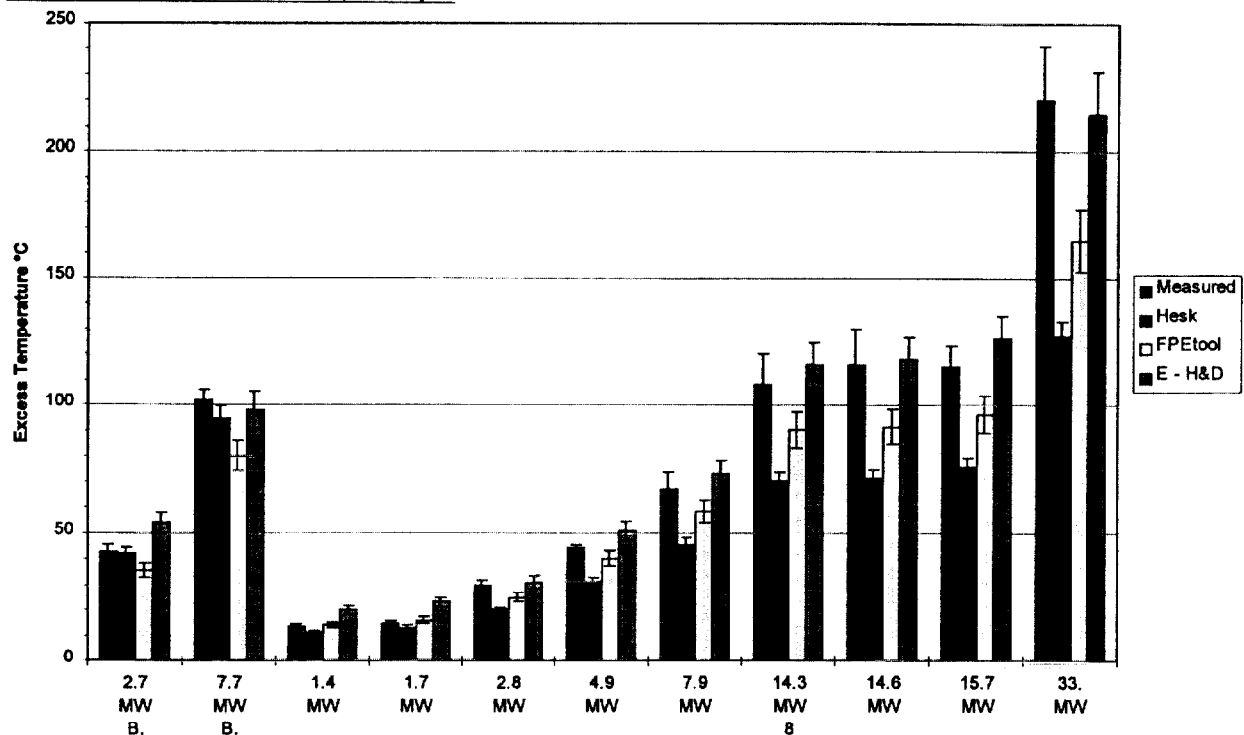


Figure 3. Comparison of Plume Centerline Temperature Excess Models with Experiments. Uncertainty intervals shown for the measured values are one standard deviation based on a least squares average of five data points taken during a twenty second interval. Uncertainty intervals shown for model squares are based on the impact of the estimated uncertainty in the HRR and radiative fraction on the calculated results. The measured value is given first followed by the Model predictions of Heskestad, FPEtool, and E - H&D.

couple located 0.3 m below the ceiling. These intervals represent the scatter in the measurements which come from a combination of plume sway and fire puffing. A small amount of electronic noise is also included in the intervals. The movement or sway of the plume at the ceiling could be determined by comparing the symmetry of the temperatures measured by the four thermocouples located 0.31 m below the ceiling in the north, south, east and west directions at 1.5 m from fire center at Barbers Point and at 3.0 m from fire center at Keflavik. For the measurements reported here, the plume center was always located near the plume centerline thermocouple based on symmetry. A detailed description of the plume motion during each of the experiments is available in Ref. [1]. Here, both video and thermocouple measurements were used to determine the lean or sway of the plume as a function of time. The deviation of the plume center at the ceiling from the geometric center of the fire source for high bay spaces has also been observed by Hinkley et. al.¹⁴ in an experimental test facility with a ceiling height of 10 m.

No radiation corrections were made to the thermocouple measurements since the smoke surrounding the thermocouples made the environment optically thick. While the absolute uncertainty in thermocouple measurements as reported by the manufacturer is $\pm 2^\circ\text{C}$, at the start of each experiment, the thermocouples used in the analysis registered the same ambient temperature to within 1°C .

Three of the fire tests conducted at Keflavik were 3.0 m square pans fires, two JP-5 and one JP-8 fires. These three tests provided an indication of repeatability for the experiments in that the average heat release rates for the three tests were 14.8 ± 0.7 MW or a repeatability of $\pm 5\%$. While JP-8 has a lower flash point than JP-5, the cone calorimeter tests for the two fuels indicated that their heat release rates were identical within the uncertainty of the cone calorimeter.¹ Therefore, the JP-8 test was included with the JP-5 tests to examine repeatability.

Measurements that were used in the fire model calculations that would most affect their predic-

tions include the heat release rate and the radiative fraction as a function of pan diameter. The accuracy of the total heat release rate depends on the accuracy of the load cell and of the heat of combustion of the fuel. Uncertainties in the heat release rate were estimated to be approximately 10% for the fire tests used in this paper.¹ Adding an estimated 5% for the uncertainty in radiative fraction, the uncertainty in the convective heat release rate should be 15%. An uncertainty of 15% in the convective heat release rate would yield an uncertainty of 10% to 15% in the temperature predictions of the correlations and computer models used in this paper. The 10% uncertainty applies to the models with no layer interaction since the excess temperature scales as the convective heat release rate to the 2/3 power. For the models which include a layer interaction, sensitivity studies indicate approximately a 10% to 15% uncertainty for an uncertainty of 15% in the convective heat release rate. The uncertainty intervals shown in Fig. 3 for the model calculations represent a $\pm 5\%$ interval for Heskestad's plume theory and $\pm 7.5\%$ interval for the two computer model calculations.

The plume correlation of Heskestad predicted plume centerline temperatures to within the uncertainty intervals for the 1.4 MW and 1.7 MW fires at Keflavik and the 2.7 MW fire at Barbers Point. The plume centerline temperatures of the larger fires were all underpredicted by this correlation. This was expected as the Heskestad correlation is based on experiments where no layer was allowed to form. Therefore, underprediction of the plume centerline temperature was expected with the best agreement occurring for the smallest fires where only a relatively cool layer would be expected to form.

The method of Evans, as implemented in FPEtool, provided poor agreement with the measurements for the large fires at both Barbers Point and Keflavik. It should be noted that the ambient temperature in FPEtool's Fire Simulator is fixed at 21°C. Including the proper ambient temperature in Fire Simulator would improve the Barbers Point simulations but increase the discrepancy of the Keflavik simulations. One reason for the underprediction of the plume centerline temperature using FPEtool comes from the way the algorithm is implemented in Fire Simulator. The values for the upper layer fire source

and ceiling height, Eqs. 4-8, are put into a correlation developed by Alpert.¹⁵ The temperature computed using this correlation at $r/H=0.18$ is the temperature used in FPEtool for all radial positions $\leq 0.18 H$. This behavior is in conflict with the observations found in these experiments and also in the experimental data set which generated the correlation of Heskestad and Delichatsios.⁷ Both of these data sets showed that the plume temperature increased as the distance from plume center decreased with the temperature at $r/H=0.18$ being substantially lower than at plume center.

The method of Evans as implemented in LAVENT predicted the plume centerline temperature to within the uncertainties of the measurement for all the large heat release rate experiments but overpredicted the centerline temperature for the smallest heat release rate experiments. One reason for this may be that in Evans' method, a term in the denominator of Eq. 5, $(\xi-1)$, approaches zero as the upper layer temperature approaches ambient temperature. The upper layer temperature calculation becomes critical for small fire sizes where the layer temperature is close to ambient.

CONCLUSION

Based on the comparisons of the model predictions of FPEtool Version 3.2, and JET, the following conclusions may be drawn.

1. The correlation of Heskestad gave predictions which agreed with the measurements when hot layers did not form. Once a hot layer formed, this correlation substantially underpredicted plume centerline temperature. In typical compartment fires with limited ventilation, models based on this correlation may yield unacceptable results.
2. As presently configured, the fire simulator portion of FPEtool will underpredict the plume centerline temperature. The fire simulator portion of FPEtool does attempt to account for the presence of a layer by using Evans' method when the layer exceeds a thickness equal to 0.12 of the fire to ceiling height but assumes that the plume temperature will be constant for distances inside $r/H=0.18$.

3. The importance of including both the entrainment of upper layer gases and a radiative fraction which is a function of fire diameter has been demonstrated in the predictions of the plume centerline temperature. Excluding either effect will cause fire models to underpredict the plume centerline temperature for large fires.

ACKNOWLEDGMENTS

We gratefully acknowledge the support of the National Aeronautics and Space Administration for their support of this project. Their support over the past three years has led to a substantial improvement in the capability of computer fire models to model detector performance in high bay structures.

We would also like to thank the Naval Facilities Engineering Command, especially Joseph E. Gott, for the use of the high bay data prior to publication.

NOMENCLATURE

C_T	9.115 (dimensionless)
D	Fire diameter (m)
c_p	Heat capacity of ambient gas (kJ/kg °C)
g	Acceleration of gravity (m/s ²)
H	Height of ceiling above fire (m)
Q	Total heat release rate (kW)
Q_c	Convective heat release rate (kW)
Q_i	Strength of substitute source (dimensionless)
r	Radial distance from plume center (m)
T_u	Upper layer temperature
T_∞	Ambient temperature (°C)
ΔT	Excess temperature (°C)
ΔT_p	Excess plume centerline temperature (°C)
y_L	Upper layer thickness (m)
z	Height above the fire surface (m)
$Z_{1,1}$	Height of the fire to the layer interface (m)
$Z_{1,2}$	Height of the substitute source to the layer interface (m)
z_0	Location of the virtual origin (m)
β	Velocity to temperature ratio of Gaussian profile half widths (dimensionless)

ξ	Ratio of upper to lower layer temperature (dimensionless)
ρ_x	Ambient gas density (kg/m ³)
χ_r	Radiative fraction (dimensionless)

REFERENCES

1. Gott, J.E., Lowe, D.L., Notarianni, K.A. and Davis W.D., "Analysis of High Bay Hangar Facilities for Fire Detector Sensitivity and Placement," *National Institute of Standards and Technology*, NIST TN 1423, 1997, pp. 1-315.
2. Deal, S., "Technical Reference Guide for FPEtool, Version 3.2," *National Institute of Standards and Technology*, NISTIR 5486-1, 1995, pp. 1-127.
3. Morton, B.R., Taylor, B.I. and Turner, J.S., "Turbulent Gravitational Convection from Maintained and Instantaneous Sources," *Proc. Roy. Soc.* A234, 1956, pp. 1-23.
4. Heskestad, G., "Engineering Relations for Fire Plumes," *Fire Safety Journal*, Vol. 7 1984, pp. 25-32.
5. Cooper, L.Y., "Estimating the Environment and the Response of Sprinkler Links in Compartment Fires with Draft Curtains and Fusible Link-Actuated Ceiling Vents - Part I: Theory," *National Institute of Standards and Technology*, NBSIR 88-3734, 1988, pp. 1-32.
6. Evans, D.D., "Calculating Sprinkler Actuation Time in Compartments," *Fire Safety Journal*, Vol. 9, 1985, pp. 147-155.
7. Heskestad, G. and Delichatsios, M.A., "The Initial Convective Flow in Fire," *17th International Symposium on Combustion*, Combustion Institute, Pittsburgh, PA, 1978, pp. 1113-1123.
8. Yang, J.C., Hamins, A. and Kashiwagi, T., "Estimate of the Effect of Scale on Radiative Heat Loss Fraction and Combustion Efficiency," *Combustion Science and Technology*, Vol. 96, 1994, pp. 183-188.
9. Souil, J.M., Vantelon, J.P., Joulain, P. and Grosshandler, W.L., "Experimental and The-

- oretical Study of Thermal Radiation from Freely Burning Kerosene Pool Fires," *Progress in Astronautics & Aeronautics* (J. R. Bowen, J.-L. Leyer, and R. I. Solenkhin, Eds.), AIAA Vol. 105, 1986, pp. 388–401.
10. Koseki, H. and Yumoto, T., "Air Entrainment and Thermal Radiation from Heptane Pool Fires," *Fire Technology*, Vol. 24, 1988, pp. 33–47.
 11. Koseki, H., "Combustion Properties of Large Liquid Pool Fires," *Fire Technology*, Vol. 25, 1989, pp. 241–255.
 12. Mudan, K.S. and Croce, P.A., "Fire Hazard Calculations for Large Open Hydrocarbon Fires", *SFPE Handbook for Fire Protection Engineering 2 ed.*, National Fire Protection Association, Quincy, MA, 1995, pp. 3-208—3-209.
 13. Davis, W.D. and Cooper, L.Y., "Estimating the Environment and the Response of Sprinkler Links in Compartment Fires with Draft Curtains and Fusible Link-Actuated Ceiling Vents—Part II: User Guide for the Computer Code LAVENT," *National Institute of Standards and Technology*, NISTIR 89-4122, 1989, pp. 1–36.
 14. Hinkley, P.L., Hansell, G.O., Marshall, N.R. and Harrison, R., "Large-Scale Experiments with Roof Vents and Sprinklers Part 1: Temperature and Velocity Measurements in Immersed Ceiling Jets Compared with a Simple Model", *Fire Science and Technology*, Vol. 13, 1993, pp. 19–41.
 15. Alpert, R.L., "Calculation of Response Time of Ceiling-Mounted Fire Detectors," *Fire Technology*, Vol. 8, 1972, pp. 181–195.